Available online at www.sciencedirect.com

ScienceDirect

ARTICLE

# Spheroidizing Behavior of the Lamellar Al$_8$CeCu$_4$ Phase in Al-14Cu-7Ce Alloy

Li Hai[1,2],     Xu Wei[1],     Wang Zhixiu[1,2],     Fang Bijun[1],     Song Renguo[1,2],     Zheng Ziqiao[3]

[1] *Changzhou University, Changzhou 213164, China;* [2] *Jiangsu Key Laboratory of Materials Surface Technology, Changzhou 213164 China;*

[3] *Central South University, Changsha 410083, China*

**Abstract:** The spheroidizing behavior of the lamellar Al$_8$CeCu$_4$ phase in the Al-14Cu-7Ce alloy annealed at elevated temperatures was investigated by microstructure observation, hardness testing and theoretical calculation. Results show that with increasing the annealing temperature, the spheroidizing process of the Al$_8$CeCu$_4$ phase is accelerated. The controlling element for the spheroidizing process is determined to be Ce by theoretical calculation using the general rate equation. Microstructure observation indicates that the spheroidizing process of the Al$_8$CeCu$_4$ phase includes two successive steps, i.e., the curved lamella breaking into long rods by Gibbs-Thompson effect and then the rods separating into spherical particles further by Rayleigh's capillary induced perturbation mechanism.

**Key words:** aluminum alloy; Al$_8$CeCu$_4$ phase; spheroidizing

Two-phase of lamellar structures are commonly observed in metallic materials, e.g. pearlitic steels[1,2] and $\alpha+\beta$ titanium alloys[3,4]. These materials have relatively higher mechanical properties than those with spherical second-phase particles. Spherical particles can be achieved by spheroidizing annealing at elevated temperatures, which reduces the hardness of the materials and improves the machinability. Furthermore, when the materials serve at elevated temperatures, the lamellar phase will spheroidize spontaneously due to its high interface energy, which inevitably causes the instability of mechanical properties. Therefore, it is important to clarify the spheroidizing behavior of the lamellar phase at elevated temperatures to meet the requirement of applications.

As a heat-resistant and cast Al alloy, the Al-14Cu-7Ce alloy has attracted wide attention recently[5-10]. According to the Al-Ce-Cu ternary phase diagram[8], the Al-14Cu-7Ce alloy belongs to the pseudo-binary Al-Al$_8$CeCu$_4$ eutectic composition, which implies that the alloy has good castability due to extremely narrow solidification temperature range. Previous studies have indicated that the as-cast Al-14Cu-7Ce alloy has good elevated temperature mechanical properties due to the presence of fine and lamellar Al$_8$CeCu$_4$ phase[6-8]. Both good heat resistance and castability of the Al-14Cu-7Ce alloy make it potential to use at elevated temperatures. The objective of the present study is to investigate the spheroidizing behavior and mechanism of the lamellar Al$_8$CeCu$_4$ phase in the Al-14Cu-7Ce alloy.

## 1 Experiment

The alloy castings, with the chemical composition (wt%), of 14 Cu, 7 Ce and balance of Al were prepared in the laboratory. Slices of 10 mm × 10 mm × 3 mm were machined and then annealed for different time at 743, 783, 823 and 863 K. Vickers hardness was measured on a HVS-5Z unit with a load of 500 g. The presented hardness was the average of at least 10 testing points.

Microstructure observation was performed on a XJG-05 optical microscopy (OM). A TCI-1000 image processing

software was used to characterize the spheroidizing process of the lamellar $Al_8CeCu_4$ phase quantitatively. Here, the criterion of aspect ratio value of 3 was adopted to determine whether the $Al_8CeCu_4$ phase was spheroidized [11]. When the volume fraction of the spheroidized $Al_8CeCu_4$ particles in the Al-14Cu-7Ce alloy exceeded 95%, the spheroidizing process was regarded as finishing. The JSM-6510 scanning electron microscopy (SEM) and XJG-05 optical microscopy were used to analyze the morphology evolution of the $Al_8CeCu_4$ phase and to determine the spheroidizing mechanism.

## 2　Results and Discussion

### 2.1　Effect of annealing temperature and time on spheroidizing process of the lamellar $Al_8CeCu_4$ phase

Fig.1 shows the microstructures of the Al-14Cu-7Ce alloy with their corresponding aspect ratio distribution histograms of the $Al_8CeCu_4$ phase. The typical as-cast microstructures of the alloy are characterized by the lamellar $Al_8CeCu_4$ phases (black and curved) in the Al matrix (white), as shown in Fig.1a. The inserted distribution histograms indicate that the aspect ratio of the $Al_8CeCu_4$ phase is in the range of 1 to 17 and the spheroidization fraction is below 3%.

Fig.1b~1e present the microstructures of the Al-14Cu-7Ce alloy annealed for 8 h at 743, 783, 823, and 863 K, respectively. Fig.2 further shows the volume fraction variation of the spheroidized $Al_8CeCu_4$ phase with the annealing time at the four temperatures. The volume fractions of the spheroidized $Al_8CeCu_4$ phase are 5.7%, 8.7%, 58.6% and 98.7%, respectively, with the increase of the annealing temperature from 743 to 863 K, indicating the acceleration of the spheroidizing rate with increasing the annealing temperature.

From Fig.2, the completing time of the spheroidization of the $Al_8CeCu_4$ phase is determined as 120, 72, 36 and 8 h at 743, 783, 823 and 863 K, respectively. At the same time, the average radius of the spheroidized $Al_8CeCu_4$ particles increases and their number density decreases with increasing the annealing temperature, which can be seen by comparing Fig.1e and 1f. The spheroidization completing time, average radius and number density of the $Al_8CeCu_4$ phase during annealing at four temperatures are listed in Table 1.

### 2.2　Determination of the controlling element during spheroidizing

Spheroidizing process of second-phase particles is closely related to atomic diffusion. In order to clarify the spheroidizing behavior of the lamellar $Al_8CeCu_4$ phase, it is necessary to determine the spheroidizing process controlled element. The hardness of the Al-14Cu-7Ce alloy is closely related to the spheroidizing process of the $Al_8CeCu_4$ phase, which belongs to the thermal activation process. Therefore, the well-known rate equation can be used to determine the controlling element [11]:
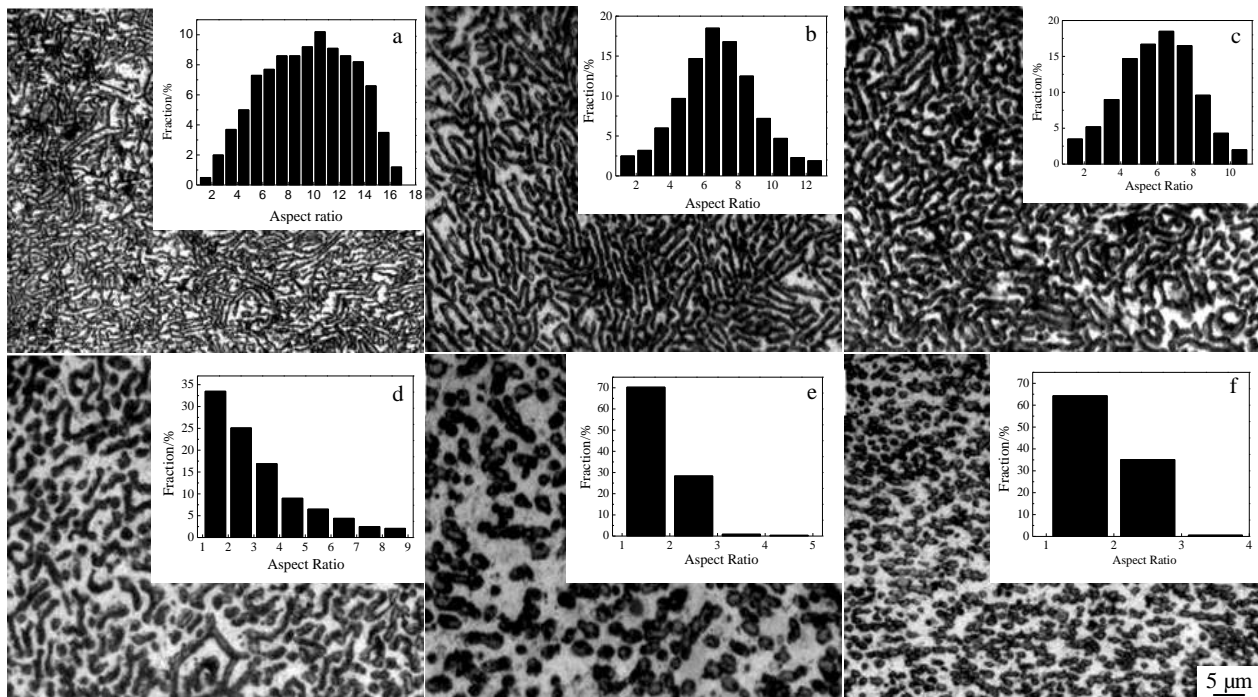


Fig.1　OM microstructures of Al-14Cu-7Ce alloy and the corresponding aspect ratio distribution of $Al_8CeCu_4$ phase as-cast (a) and annealing at 743 K (b), 783 K (c), 823 K (d), 863 K (e) for 8 h; 823 K (f) for 72 h
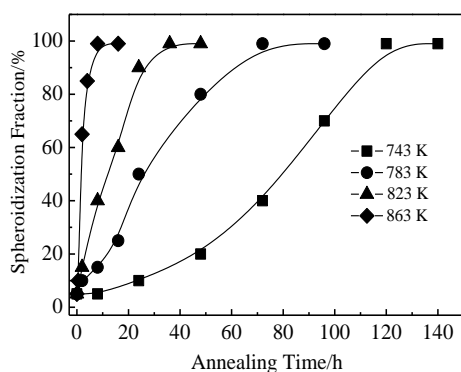
Fig.2 Volume fraction variation of the spheroidized $Al_8CeCu_4$ phase annealed at four temperatures for different time
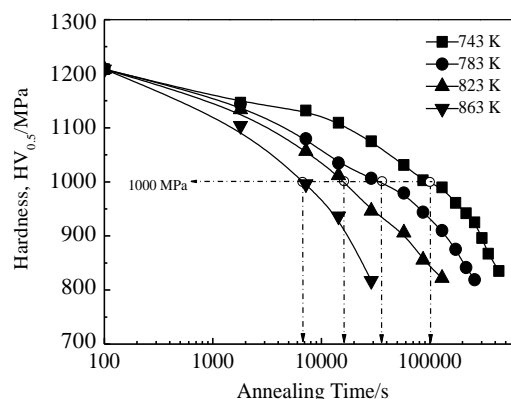


Fig.3 Hardness variation of the Al-14Cu-7Ce alloy with annealing time at four temperatures

**Table 1 Spheroidization completing time, mean radius and number density of the $Al_8CeCu_4$ phase annealed at four temperatures**

| Temperature/K | Spheroidization completing time/h | Mean radius/ $\mu m$ | Number density/ $\times 10^5$ $mm^{-2}$ |
|---|---|---|---|
| 743 | 120 | 1.2 | 4.4 |
| 783 | 72 | 1.7 | 3.1 |
| 823 | 32 | 2.1 | 2.4 |
| 863 | 8 | 4.3 | 1.2 |

$$\ln t = A + Q/RT \qquad (1)$$

where, $t$ is annealing time, $Q$ is diffusion activation energy, $R$ is ideal gas constant, $T$ is annealing temperature and $A$ is a constant. That is, the natural logarithm of the annealing time ($\ln t$) for the initial mechanical properties of the alloy decreases to the same value at different annealing temperatures and the reciprocal of the annealing temperatures ($1/T$) meets the linear relationship.

The hardness variation of the Al-14Cu-7Ce alloy annealed at 4 temperatures is shown in Fig.3. According to Fig.3, the time needed for the hardness HV of the Al-14Cu-7Ce alloy decreasing from the initial 1208 MPa to 1000 MPa is $6.7 \times 10^3$, $1.6 \times 10^4$, $2.6 \times 10^4$ and $1.1 \times 10^5$ s for the annealing temperature 743, 783, 823 and 863 K, respectively. Then, the linear fitting plot of $\ln t$ vs. $1/T$ is obtained in Fig.4, in which its slope $Q/R = 14.2$ and the calculated $Q = 118.5$ kJ/mol. The $Q$ value is smaller than the self-diffusion activation energy of Al ($Q_{Al} = 142.3$ kJ/mol)[12] and the volume diffusion activation energy of Cu in the Al matrix ($Q_{Cu} = 133.9$ kJ/mol) [13], whereas close to the volume diffusion activation energy of Ce in the Al matrix ($Q_{Cu} = 115.6$ kJ/mol) [14].

It is known that the diffusion constants of Al, Cu and Ce in the Al matrix are $D_{0Al} = 1.7 \times 10^{-4}$ [12], $D_{0Cu} = 4.4 \times 10^{-5}$ [13] and $D_{0Ce} = 6.7 \times 10^{-10}$ $m^2/s$ [14], respectively. Based on the Arrhenius relationship:

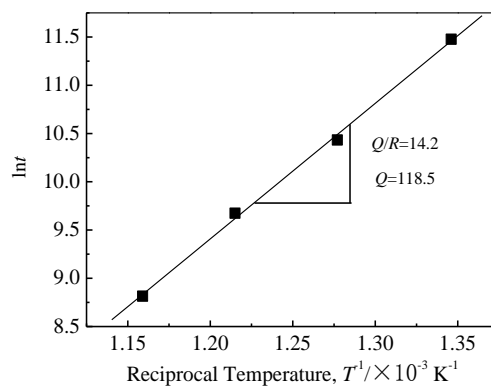$$D = D_0 \exp(-Q/RT) \qquad (2)$$



Fig.4 Plot of $\ln t$ vs $1/T$

**Table 2 Diffusion coefficients of Al, Cu and Ce in the Al matrix at different annealing temperatures**

| Temperature/ K | Diffusion coefficient/$m^2$ $s^{-1}$ | | |
|---|---|---|---|
| | $D_{Al}/\times 10^{-13}$ | $D_{Cu}/\times 10^{-13}$ | $D_{Ce}/\times 10^{-17}$ |
| 743 | 0.156 | 0.177 | 0.500 |
| 783 | 0.504 | 0.544 | 1.30 |
| 823 | 1.45 | 1.50 | 3.08 |
| 863 | 3.78 | 3.78 | 6.75 |

where, the diffusion coefficients of Al, Cu and Ce in the Al matrix at four annealing temperatures are calculated and listed in Table 2. It is clearly seen that the value of $D_{Ce}$ is far smaller than that of $D_{Al}$ or $D_{Cu}$. Therefore, it is easily concluded that Ce is the spheroidizing process controlled element of the $Al_8CeCu_4$ phase.

### 2.3 Spheroidization process of $Al_8CeCu_4$ phase

The SEM morphologies of the $Al_8CeCu_4$ phase annealed at 823 K for different times are shown in Fig.5. To clarify the morphologies of the $Al_8CeCu_4$ phase, the Al-14Cu-7Ce alloy was deeply etched in 10% NaOH solution for 15 min, aiming to remove the Al matrix and retain the $Al_8CeCu_4$
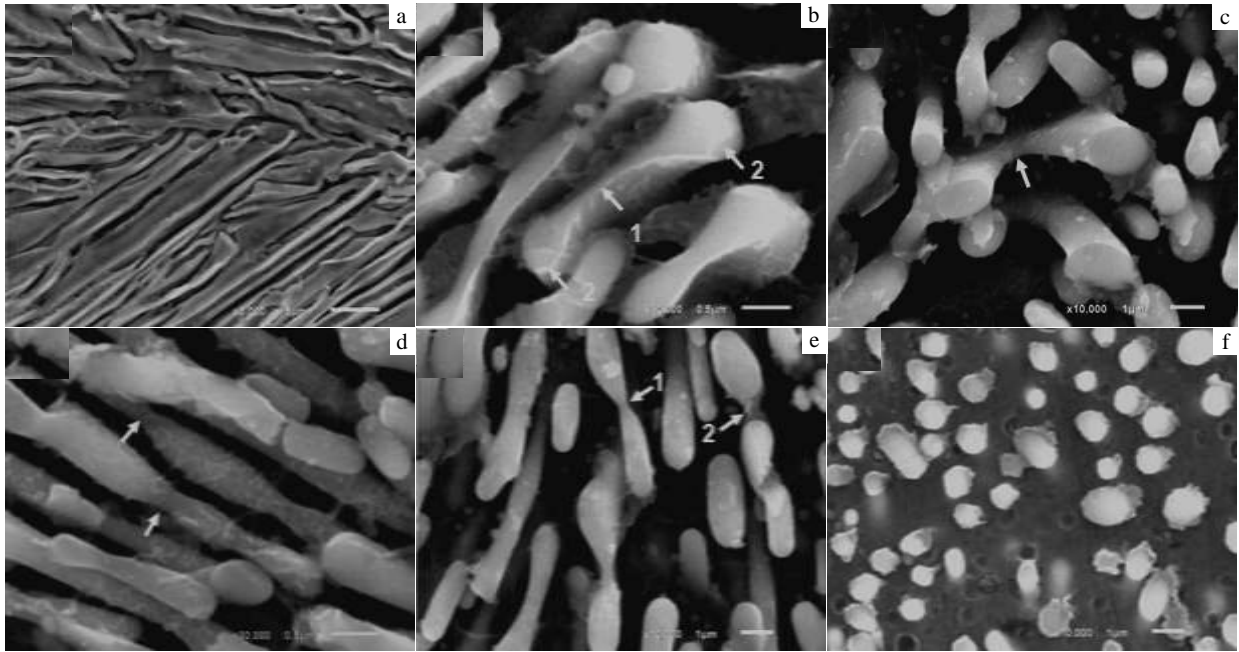
Fig.5　SEM morphologies of the $Al_8CeCu_4$ phase in the Al-14Cu-7Ce alloy annealed at 823 K for different time: (a) 0 h (as-cast), (b) 4 h, (c) 8 h, (d) 16 h, (e) 24 h, and (f) 36 h

phase. Fig.5a shows that the $Al_8CeCu_4$ lamellae in the as-cast Al-14Cu-7Ce alloy are narrow and curved. After annealing at 823 K for 4 h, the lamellae thin at the center (arrow "1") and widen at two end sides (arrow "2"), as shown in Fig.5b. Increasing annealing time to 8 h, the $Al_8CeCu_4$ lamellae begin to spin off gradually along the longitudinal direction, as arrowed in Fig.5c. Fig.5d displays that the $Al_8CeCu_4$ lamellae have split into long and round rods after annealing for 16 h accompanied by some relatively thinner sites along the longitudinal direction, as arrowed in Fig.5d. As shown in Fig.5e, when annealed at 823 K for 24 h, the thinning of the long rods at some relatively thinner sites proceeds further (arrow "1") and then they separate into shorter ones (arrow "2"). After annealing for 32 h, only spherical $Al_8CeCu_4$ particles with the diameter of 0.3~2 μm are observed as shown in Fig.5f, which indicates that the spheroidizing process of the Al-14Cu-7Ce alloy has completed.

It is well accepted that the spheroidizing process of the second-phase particles depends closely on the Gibbs-Thompson effect [14], which describes the variation of equilibrium solute concentration in the adjacent matrix around the particles with different curvatures. Obviously, the larger the curvatures of the particles, the higher the equilibrium concentration will be, which leads to a concentration difference between particles with different diameters and causes the dissolution of small particles and the growth of large particles. Based on the Gibbs-

Thompson relation, it is easy to clarify the spheroidizing process of the lamellar $Al_8CeCu_4$ phase.

As seen in Fig.5a, there are many grooves at the center of the $Al_8CeCu_4$ lamellae. During annealing at elevated temperatures, the matrix concentration around the center of the $Al_8CeCu_4$ lamella is higher than that at the two end sides due to the curvature difference. As a result, the solutes flow from the center to the two end sides, causing the thinning of the center and the widening of the two end sides (Fig.5b). Furthermore, the partial dissolution of the lamella center will produce new curvatures (Fig.5b), which in turn accelerates the dissolution of the lamella. When the dissolution proceeds along the longitudinal direction, the lamella finally splits into two long and round rods. Once the rods are formed in the matrix, the Rayleigh's capillarity induced perturbation mechanism will act [15]. This mechanism demonstrates that a long rod is intrinsically unstable and spontaneously breaks into a row of spherical particles with intervals of maximum perturbation wavelength $\lambda_{max} = 2\pi(2r)^{1/2}$, where $r$ is the radius of the rod. As arrowed in Fig.5d and 5e (arrow "1"), the rods thin gradually with increasing annealing time at 823 K, and the rods separate into shorter ones further, as arrowed in Fig.5e (arrow "2").

In summary, the spheroidizing process of the lamellar $Al_8CeCu_4$ phase is as follows: the $Al_8CeCu_4$ lamellae first break into the long and round rods due to the Gibbs-Thompson effect. And then, the long rods divide into short

ones by the Rayleigh's capillarity induced perturbation mechanism. Finally, the short rods transform into spherical particles.

## 3 Conclusions

1) The spheroidizing process of the lamellar $Al_8CeCu_4$ phase in the Al-14Cu-7Ce alloy is accelerated with the increasing of annealing temperature. Such process is controlled by the volume diffusion of Ce in the Al matrix.

2) The spheroidizing process of the lamellar $Al_8CeCu_4$ phase obeys such sequences: the $Al_8CeCu_4$ lamellae are divided into long rods along the grooves firstly; then the rods break into shorter rods; finally, the short rods further spheroidize.

## References

1 Chen W, Li L, Yang W *et al. Acta Metallurgica Sinica*[J], 2009, 45(1): 151 (in Chinese)

2 Chen W, Li L, Yang W *et al. Acta Metallurgica Sinica*[J], 2009, 45(1): 156 (in Chinese)

3 Park C H, Won J W, Park J W *et al. Metallurgical Materials Transaction A*[J], 2012, 43: 977

4 Poths R M, Wynne B P, Rainforth W M *et al. Metallurgical Materials Transaction A*[J], 2004, 35: 2993

5 Li W, Li H, Wang Z *et al. Materials Science Engineering A*[J], 2011, 528: 4098

6 Huang L, Li H, Wang Z *et al. Transactions of Materials and Heat Treatment*[J], 2012.33: 60

7 Belov N A, Khvan A V, Alabin A N. *Materials Science Forum*[J], 2006, 519-521: 395

8 Belov N A, Khvan A V. *Acta Materials*[J], 2007, 55: 5473.

9 He B, Jin S, Zhang L G *et al. Journal of Alloys and Compound*[J], 2009, 484: 286

10 Li Hai, Xu Wei, Wang Zhixiu *e al. Rare Metal Materials and Engineering*[J], 2016, 45(5): 1106

11 Tian Y L, Kaft R W. *Metallurgical Transaction A*[J], 1987, 18: 1403

12 Lavernia E J, Ayers J D, Srivatsan T S. *International Materials Review*[J], 1992, 37: 1

13 Du Y, Chang Y A, Huang B *et al. Materials Science Engineering A*[J], 2003, 363: 140

14 Cai W P. *Journal of Materials Science Letter*[J], 1997: 1824

15 Nichols F A. *Journal of Materials Science*[J], 1976, 11: 1077

# Al-14Cu-7Ce 合金中片状 Al₈CeCu₄ 相的球化行为研究

李 海 [1,2]，许 伟 [1]，王芝秀 [1,2]，方必军 [1]，宋仁国 [1,2]，郑子樵 [3]

(1. 常州大学，江苏 常州 213164)

(2. 江苏省材料表面技术重点实验室，江苏 常州 213164)

(3. 中南大学，湖南 长沙 410083)

摘 要：通过微观组织观察、硬度测试和理论计算，研究了 Al-14Cu-7Ce 合金中片状 $Al_8CeCu_4$ 相的高温球化行为。实验结果表明，随着退火温度的升高，$Al_8CeCu_4$ 相的球化速度加快；采用通用速率公式计算出 $Al_8CeCu_4$ 相的球化过程控制元素为 Ce；微观组织观察表明，$Al_8CeCu_4$ 相球化过程包括 Gibbs-Thompson 效应作用下片状 $Al_8CeCu_4$ 相首先分解成棒状 $Al_8CeCu_4$ 相，随后在 Rayleigh 毛细管扰动机制作用下进一步分解成球状 $Al_8CeCu_4$ 相。

关键词：铝合金； $Al_8CeCu_4$ 相；球化

作者简介：李 海，男，1972 年生，博士，教授，常州大学材料科学与工程学院，江苏 常州 213164，电话：0519-86330069，E-mail: lehigh_73@163.com